Urania
Jurnal Ilmiah Daur Bahan Bakar Nuklir

Beranda jurnal: http://jurnal.batan.go.id/index.php/urania/

OXIDE LAYER CHARACTERIZATION OF AlMg2 CLADDING OF IRRADIATED U_3Si_2/Al FUEL WITH 4.8 gU/cm^3 DENSITY

Juan Carlos Sihotang[1], Maman Kartaman Ajiriyanto[1], Ely Nurlaily[2], Junaedi[2], Aslina Br. Ginting[1]
[1]Research Center for Nuclear Fuel Cycle and Radioactive Waste Technology
Kawasan Sains dan Teknologi B. J. Habibie Gedung 20, Tangerang Selatan, Banten 15314
[2] Directorate for Development of Nuclear Facilities
Kawasan Sains dan Teknologi B. J. Habibie Gedung 30, Tangerang Selatan, Banten 15314
e-mail: juancarlossihotang@brin.go.id

(Naskah diterima: 12–09–2022, Naskah direvisi: 29–09–2022, Naskah disetujui: 04–10–2022)

ABSTRACT

OXIDE LAYER CHARACTERIZATION OF AlMg2 CLADDING OF IRRADIATED U_3Si_2/Al FUEL WITH 4.8 gU/cm^3 DENSITY. To investigate the performance of AlMg2 cladding in the U_3Si_2/Al dispersion fuel, oxide layer characterization of AlMg2 cladding of the irradiated U_3Si_2/Al fuel with 4.8 gU/cm^3 density was conducted. The oxide layer on the surface of AlMg2 cladding is one of the changes that occur on the cladding after the U_3Si_2/Al fuel plate has been irradiated in the RSG-GAS reactor to a burn-up of ~40%. The characterization and observation of the oxide layer was conducted using SEM (Scanning Electron Microscope) and Energy-dispersive X-ray spectroscopy (EDS). Samples with a size of 3x3 mm were taken from the middle of the fuel plate (middle position). After cutting, metallographic preparation includes mounting, grinding, polishing, and ultrasonic cleaning. SEM preparation was carried out by sputter coating using Au layer. The oxide layer on the AlMg2 cladding has a thickness of 10.3 µm with a uniformly distributed cracks along the oxide layer.

Keyword: LEU, uranium-silicide, post-irradiation examination, AlMg2 cladding, oxide layer.

ABSTRAK

KARAKTERISASI LAPISAN OKSIDA KELONGSONG AlMg2 BAHAN BAKAR U_3Si_2/Al PASCAIRADIASI DENSITAS 4,8 gU/cm^3. *Dalam rangka mengetahui unjuk kerja kelongsong AlMg2 pada bahan bakar dispersi U_3Si_2/Al, dilakukan karakterisasi lapisan oksida pada kelongsong AlMg2 pada pelat bahan bakar U_3Si_2/Al densitas 4,8 gU/cm^3 pascairadiasi. Lapisan oksida pada permukaan kelongsong AlMg2 merupakan salah satu perubahan yang terjadi pada kelongsong setelah pelat bahan bakar U_3Si_2/Al mengalami iradiasi di dalam reaktor RSG-GAS hingga fraksi bakar 40%. Karakterisasi dan pengamatan lapisan oksida dilakukan dengan menggunakan SEM (*scanning electron microscope*)* dan *EDS* (Energy-dispersive X-ray spectroscopy)*. Sampel dengan ukuran 3x3 mm diambil dari bagian tengah pelat (posisi* middle*). Setelah pemotongan, preparasi metalografi dimulai dari mounting, pengamplasan, pemolesan, hingga pencucian. Preparasi SEM dilakukan dengan* sputter coating *menggunakan lapisan Au. Lapisan oksida pada kelongsong AlMg2 yang memiliki ketebalan 10.3 µm dengan retakan yang terdistribusi seragam di sepanjang lapisan oksida.*

Kata kunci*: LEU, uranium silisida, uji pascairadiasi, kelongsong AlMg2, lapisan oksida.*

DOI: https://doi.org/10.17146/urania.2022.28.3.6755

INTRODUCTION

Reaktor Serba Guna G.A. Siwabessy (RSG-GAS, formerly named MPR-30) is an Indonesian multipurpose research reactor operated by Badan Tenaga Nuklir Nasional (National Nuclear Energy Agency/BATAN) located at PUSPIPTEK Tangerang Selatan, Indonesia. It is a 30 MWth maximum power pool-type reactor with light water as coolant and moderator, and beryllium as the neutron reflector. The reactor was designed for material testing, radioisotopes production, activation analysis, neutron physics measurements and silicon doping production. The first criticality was achieved on July 29, 1987. The reactor uses the plate-type fuel element (FE), which initially was low enriched uranium (LEU; 19.75 w/o U-235 enrichment) U_3O_8 fuel dispersed in the Al matrix with uranium density of 2,96 gU/cm^3. However, in 1999 the whole reactor core of the RSG-GAS converted from using U_3O_8/Al fuel into using silicide fuel (U_3Si_2/Al) domestically produced to allow optimization of reactor utilization. At present, RSG-GAS uses LEU U_3Si_2/Al fuel with uranium density 2,96 g/cm^3. It has an average thermal neutron flux of 2.5 x 10^{14} n/cm^2 s. On the 10x10 core grid positions there are 40 standard fuel elements (each consists of 21 fuel plates), 8 control elements (each consists of 15 fuel plates to provide a space for the control rods), Be reflector elements, and other irradiation facilities [1]–[10].

Following the success in utilizing the 2,96 gU/cm^3 U_3Si_2/Al fuel, BATAN continue to develop U_3Si_2/Al fuel with higher uranium density. Experimental mini and full scale U_3Si_2/Al fuel with density 4,8 gU/cm^3 had been successfully fabricated in PTBBN BATAN with fabrication process that is almost similar with U_3O_8/Al fuel [11]. The uranium-silicide fuel plate is produced by melting uranium and silicon (92,5% and 7,5% by weight) together to make U_3Si_2 ingot, followed by comminution (milling) to produce a powder. The silicide powder is mixed with aluminum powder with ratio according to the uranium density, and then pressed into a powder metallurgical compact. The compact is then clad by a frame and two cover sheets of aluminium-magnesium alloy (AlMg2), and welded on some spot on the four side, before hot and cold rolling to produce a fuel plate with thickness of 1,3 mm [12].

Three full size U_3Si_2/Al fuel plates (4,8 gU/cm^3) namely CBBJ249, CBBJ250, and CBBJ251 had been successfully manufactured by PTBBN BATAN and irradiated in the reactor at 15 MW power. The three fuel plates were inserted in a fuel bundle while the other 18 plates were dummy. Each of the three plates were irradiated at different burn-up of approximately 20, 40, and 60% [13], [14]. The irradiation time was 87 days for CBBJ 249, 175 days for CBBJ251, and 263 days for CBBJ250. Based on calculation using ORIGEN2, the amount of burned ^{235}U was 18.41% for CBBJ249, 36.71% for CBBJ251, and 55.16% for CBBJ250 [15] After irradiation and cooling down in the reactor pool, the three plates were then taken to Radiometallurgy Installation (RMI) for the post irradiation examination (PIE) to investigate the performance of the fuels. In the previous report, the microstructure of irradiated CBBJ251 (burn-up ~40%) had been successfully investigated using SEM and optical microscope, mainly the fission gas bubble formed in the fuel meat and the interaction layer between the fuel meat and Al matrix [16]. In addition to the fuel's microstructural study, investigation on the oxide layer formed on the surface of outer AlMg2 cladding of CBBJ251 fuel plate was performed using SEM-EDS analysis.

Cladding is a component of nuclear fuel elements that functions as a safety barrier and prevents contact between fuel and reactor cooling water and to prevent fission gas leakage. Inside the reactor, the cladding is a component of the nuclear fuel elements that is in direct contact with the environment for a long time [17]. During this time, the cladding and structural materials may experience damage or decrease in quality due to corrosion caused by electrochemical reactions between the surface of the cladding materials and structural materials and the environment. Severe corrosion of the nuclear fuel cladding can result in the release of fuel elements and fission products into the reactor cooling water and can have an impact on reactor safety. Therefore, the cladding material must have high corrosion resistance and other properties such as low neutron absorption cross-section, stable to irradiation, good mechanical properties, high thermal conductivity, low thermal expansion [18]. Al alloys have been used as cladding materials for U_3Si_2/Al research reactor fuels considering the properties of aluminum

suitable as cladding materials. The Al alloy used as cladding material is Al with the addition of Mg (5xxx series Al alloy) or Mg and Si (6xxx series Al alloy). ment (artificial aging). The aluminum alloy used in RSG-GAS as a U_3Si_2-Al fuel cladding is an AlMg2 alloy which has Mg content of 1.7-2.4 wt% [17].

Al alloys have high general corrosion resistance by the spontaneous formation of a protective oxide layer on the surfaces when exposed to air. However, chloride ions can attack the oxide film by absorbing on the surface of the oxide film causing different types of corrosion such as pitting corrosion, intergranular corrosion (IGC) and exfoliation corrosion [19]. Formation of oxides on the cladding can increase the fuel temperature. Because the lower thermal conductivity of the oxide than that of aluminum. Very severe corrosion on the AlMg2 cladding and accompanied by damage to the protective oxide layer can cause the release of radioactive substances from the fuel meat into the environment. In research reactors, the corrosion process is strongly influenced by operating conditions such as environmental media, pH, temperature, conductivity, and the amount of chloride ions[20].

Numerous studies have investigated the oxide layer growth on irradiated Al-based alloy cladding fuel. Kim et al [21] developed a model to predict oxide thickness on Al alloy cladding during irradiation as a function of irradiation time, cladding surface temperature, heat flux at cladding surface, coolant pH, and coolant flow rate. He also obtained the thickness data of AlMg2 cladding oxide from two irradiation tests in the ATR (Advanced Test Reactor). Oxide thickness was measured using the eddy current method at 9 locations on both sides of the plates. The predictions by the model were in good agreement with the test data from ATR, as well as with the in-pile test data from the literature.

Leenaers et al [22] observed the oxide layer on Al5754 (2.5 – 3 wt% Mg) cladding of U_3Si_2 fuel (density 5.1 and 6.1 g U/cm^3) subjected to excessive heat during irradiation (550 W/cm^2 heat flux) until the surface temperature of the cladding reached 180-200^{o}C and fuel temperature 220-240^{o}C. The oxidation of cladding started to visible at the fuel section subjected at 500 W/cm^2 where dense oxide layer formed with granular aspect of pitting corrosion. At the fuel plate section subjected to the maximum of 550 W/cm^2, the corrosion of the cladding was so severe that it formed up to the meat. The layer consisted of alumina barrier layer on top of porous boehmite (γ-AlO(OH)) bulk layer. The failure of the fuel plate was mainly caused by the degradation of cladding, not by the fuel. Low thermal conductivity of the layer increased the temperatures further and accelerated the corrosion until the cladding failed. In other study, Leenaers [23] observed the oxide layer on AlFeNi cladding from U_3Si_2 fuel (density 4.8 gU/cm^3) irradiated in the BR2 reactor under relatively severe condition until fuel burn-up of 55% and maximum temperature of the outer cladding surface of 140°C. An oxide layer with maximum thickness of 30–50 μm was found at the highest flux position. XRD analysis showed that the major constituents of the oxide were boehmite AlO(OH), bayerite $Al(OH)_3$, and aluminum. Oxide layer thickness was measured using image analysis of the SEM graph.

The objective of this study is to observe the microstructure and thickness of the oxide layer formed on the AlMg2 cladding at U_3Si_2/Al fuel density of 4.8 gU/cm^3 after being irradiated in the reactor to burn-up of 40%. Observation of the thickness of the AlMg2 cladding oxide layer on irradiated U_3Si_2/Al fuel is part of the post irradiation examination that must be carried out to understand the performance of the U_3Si_2/Al fuel.

METHODOLOGY

Uranium silicide U_3Si_2/Al fuel plate with code CBBJ251 was irradiated in RSG-GAS reactor core for 175 days. After irradiation, the fuel plate was discharged from the core to the reactor pool for cooling down for certain period of time. Then, the fuel plate was transferred to the Radiometallurgy Installation (RMI) hot cell facility for detailed post irradiation examination (PIE) through underground transfer channel. According to Kadarusmanto [15] the amount of burned ^{235}U from CBBJ251 fuel plate calculated with ORIGEN2 was 36,71%. Meanwhile, based on measurements and calculations with gamma scanning by PTBBN BATAN, the amount of burned ^{235}U was 39,42%. Nondestructive test for the plate was conducted first before cutting the fuel for the destructive test. Visual inspection and imaging with x-ray radiograph showed no

DOI: https://doi.org/10.17146/urania.2022.28.3.6755

anomalies (such as defects, blister, damage, and significant dimensional changes) were found [24].

After the nondestructive test, the plate was cut at the middle (as depicted in Fig. 1) with dimension 25 mm x 20 mm using a punching-device. The selection of this position is because highest distribution of isotopes Cs-134/Cs-137 was found in the middle position [25].

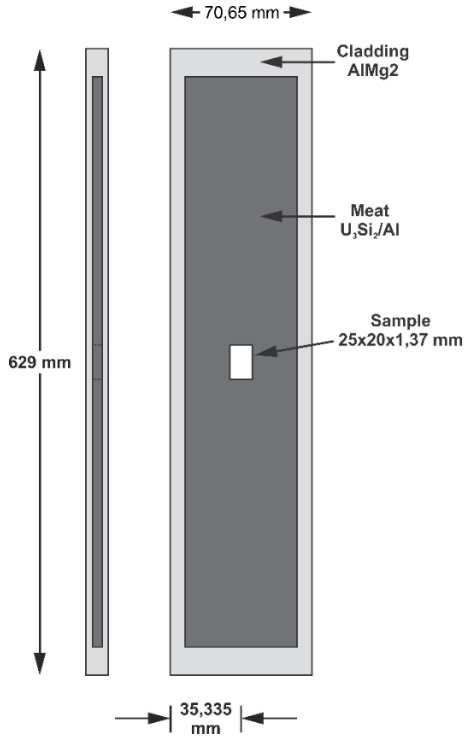

Figure 1. Sampling position in CBBJ251 fuel plate using punching-device. The dimension of the fuel plate was based on non-destructive test result [24].

The sample was cut again into smaller pieces of 3 mm x 3 mm for metallography sample using a low-speed precision cutter. Then, the sample was embedded in an epoxy resin with addition of conductive filler, in such a way that the cross-section area of the fuel can be observed. The mounted sample was mechanically wet ground with successfully finer SiC paper (up to grit 2400) and polished with 1 µm diamond paste. The polished sample was ultrasonically cleaned for about 15 minutes to clean the sample from the debris. The sample was sputter-coated with Au before microstructural characterization with SEM-EDS. SEM-EDS was performed using Phenom Pharos Desktop SEM in backscattered electron mode. The thickness of the oxide layer was measured using measurement tools in the SEM software that had been calibrated before. EDS analysis was performed to semi-quantitatively analyze the element composition on the oxide layer.

RESULTS AND DISCUSSION

The low magnifications ceramography observations of the fuel cross-section shows the oxide layer on both outer cladding surfaces of the AlMg2 cladding as shown in Figure 2(a)-(c). The detailed image of the oxide layer is shown in Figure 2(d). The formed oxide layer looks dense, non-porous, and no granular aspect appearance so that pitting corrosion is unlikely to occur, in contrast to the pitting corrosion observations by Leenaers [22] as shown in Figure 3. In Figure 2(d), the cracks are clearly visible along the oxide layer. Similar cracks on the oxide layer were also observed in the other studies [23], [26] as depicted in Figure 4. Leenaers et al [23], observed that the cracked oxide layer did not firmly attach to the irradiated AlFeNi cladding and can be removed easily. The crack pattern, as depicted in Figure 4(c), were suggested to be caused by dehydration (evaporation of the lattice water) of the oxide layer during the drying of the fuel element in the hot cell. Wintergest et al [26], who studied the corrosion product of unirradiated AlFeNi alloy obtained from autoclaves, also observed similar cracks on the oxide layer, stating that the cracks can be formed during mounting or mechanical polishing, or because of the growth stresses or thermal stresses.

The oxide layer observed in Figure 2 (d) appears as a single layer. Based on the literatures, the oxide layer on Al-based alloy cladding typically consists of all or some of protective oxide of alumina and oxide-hydrates boehmite and bayerite layer [21], [22]. Boehmite and bayerite formed in the outer surface by degradation of the alumina in the water [21]. The removed oxide layer characterized through XRD [23], also showed two major constituents of boehmite and bayerite. The temperature condition seems to affect the morphology and phase formation of the oxide layer [26]. Semi-quantitative element identification with EDS linescan showed that the layer mainly consists of Al and O atoms (Figure 5).

The thickness of the oxide layer measured using SEM image analysis software was approximately 10.3 µm. The oxide layer formed is very thin and therefore did not change the integrity of the AlMg2 cladding. As a comparison, the thickness of the AlMg2 cladding required for use in the reactor is 0.25 mm. In Leenaers' work [23], the maximum oxide layer thickness of 30–50 µm is found at the highest flux position. In the microstructural image, there are small flakes which are impurities, both from sanding grains and impurities that stick during the sample transfer process. However, these impurities do not interfere with the interpretation of microstructure images.

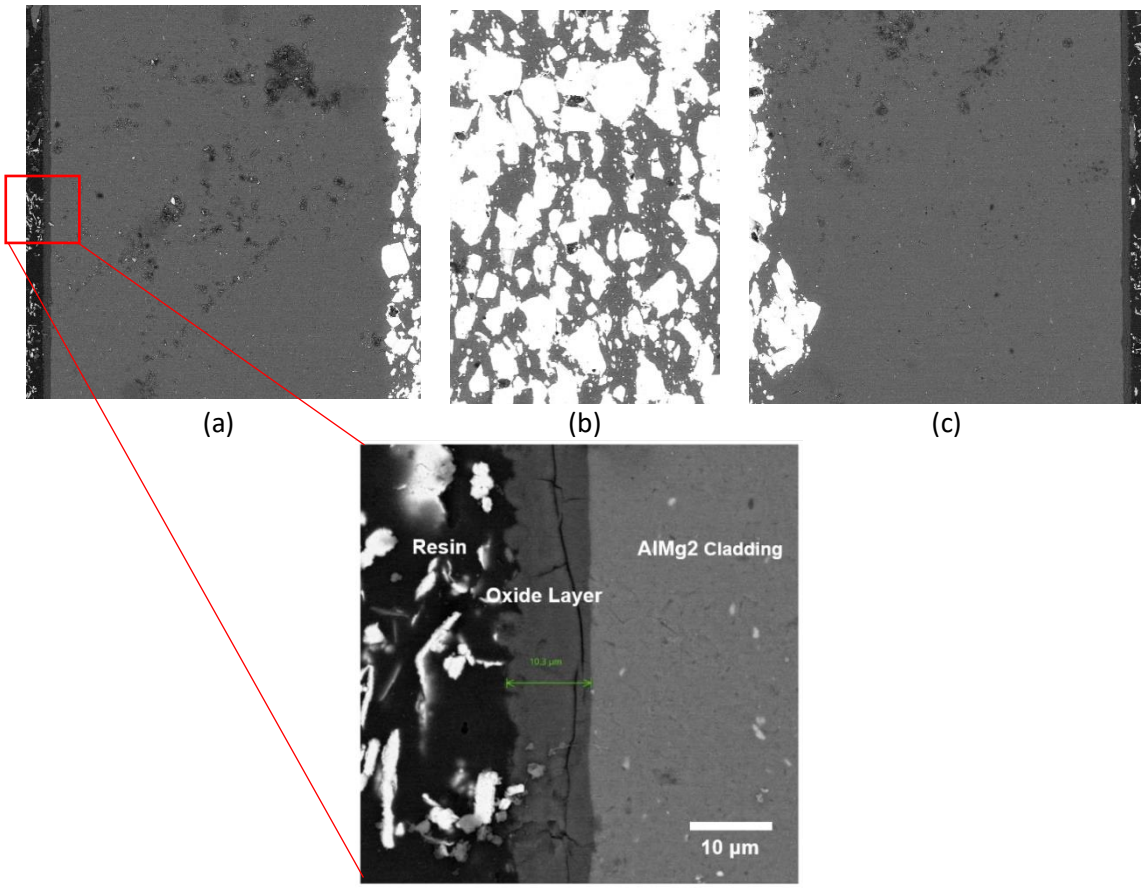

(a) (b) (c) (d)

Figure 2. Backscatter electron SEM Image of the irradiated fuel plate over the width (cross-section), showing overview of the fuel cross-section (a-c); and more detailed micrograph of the oxide layer on the fuel cladding (d).

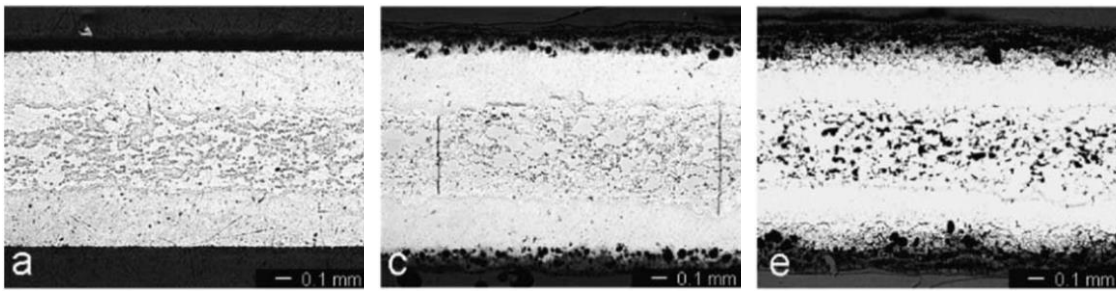

(a) (b) (c)

Figure 3. Image of the cross-section of the fuel plate submitted to ~450 W/cm^2 (a); ~500 W/cm^2 (b); and ~550 W/cm^2 (c) from Leenaers' work [22], showing granular aspect of pitting corrosion on the Al5754 alloy cladding.

DOI: https://doi.org/10.17146/urania.2022.28.3.6755

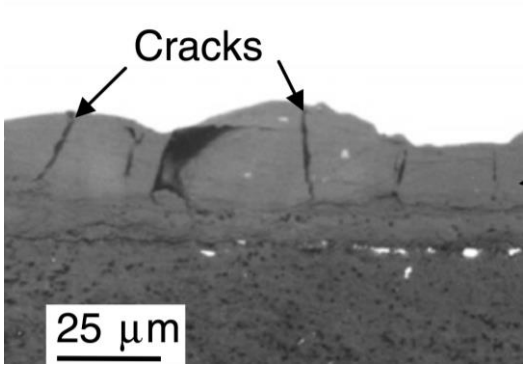

(a)

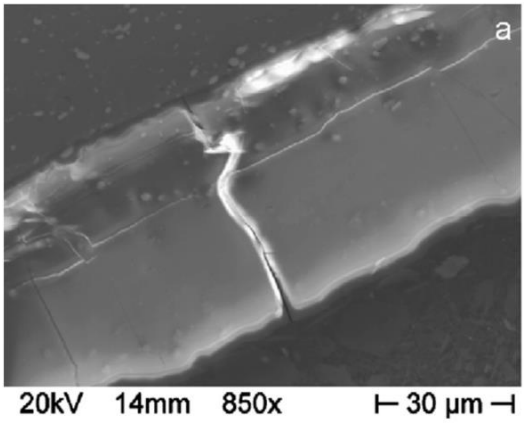

(b)

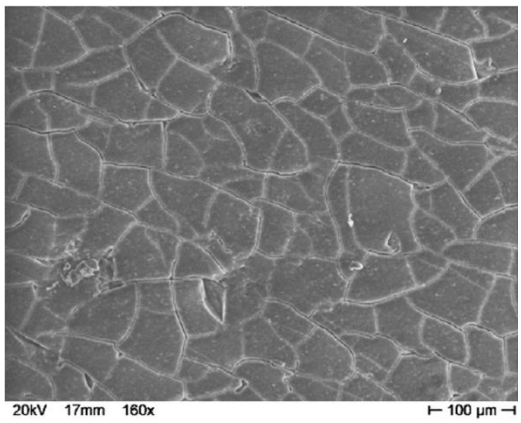

(c)

Figure 4. Micrograph showing cracks in the oxide layer of fuel cladding: AG3NE cladding in SIMONE LC-04 fuel test [21] (a), and; AlFeNi cladding from U_3Si_2 fuel [23] cross section (b) and surface (c).

The formation of an oxide layer on the metal surface is also affected by radiation. Kanjana et al [27] observed the corrosion behavior of Al 6061 immersed in demineralized water during irradiation using Co-60 gamma source for 8, 24, and 48 hours. Irradiation doses were also varied from 0 up to 4.30 kGy/hour. The results suggest that gamma radiation can accelerate the formation of the oxide layer on Al 6061 (gamma-radiation induced corrosion). Increasing the dose rate increases the density of this corrosion product. EDS analysis on the corrosion product shows the presence of Al and O.

Dian A et al [17] measured the corrosion rate of AlMg2 and AlMgSi alloys in aqueous media at pH 6.7 (according to the primary cooling water conditions of the RSG GAS reactor) and pH 2 (abnormal condition) using potensiodynamic polarization electrochemical method. Even at pH 2, the corrosion rate of AlMg2 and AlMgSi still in the safe category (<20 mpy). The study also showed thatr AlMg2 showed a better corrosion resistance compared to AlMgSi at both pH condition. During irradiation of AlMg2 alloy, due to transmutation of Al by neutron capture, Si is formed, and the alloy will evolve to an Al–Mg–Si alloy (6XXX series) [22]. In a study conducted by Febrianto et al [20], an increase in temperature (from 28 - 45°C) and an increase in chloride ion concentration (from 0.005 - 0.035 ppm NaCl) is directly proportional to the corrosion rate of AlMg2 alloy. The highest corrosion rate of AlMg2 alloy was in a solution with a concentration of 0.035 ppm NaCl and a temperature of 45°C, namely 1.23 x 10-3 mpy. Based on all the literatures above, it can be concluded that the formation of an oxide layer on the AlMg2 cladding occurs due to environmental influences in the reactor such as gamma radiation temperature, environmental pH, and the amount of chloride ions in the reactor cooling water.

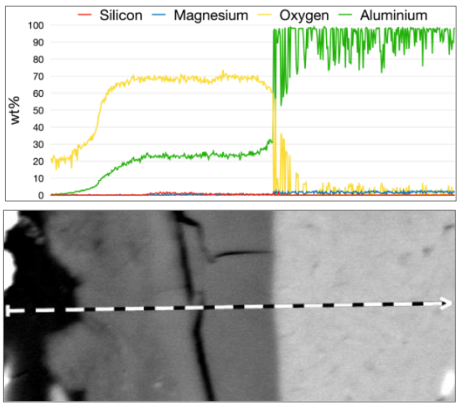

Figure 5. Semi-quantitative linescan covering the AlMg2 cladding and the oxide layer.

CONCLUSIONS

U_3Si_2/Al (4,8 gU/cm^3) fuel plates with AlMg2 cladding after irradiation in RSG-GAS reactor core for 175 days at 15 MW power and fuel burnup about 40% showed a good performance. The oxide layer formed on the surface of the AlMg2 cladding had a thickness of 10.3 µm, which is relatively thin and did not cause failure at the fuel cladding. The cracks on the oxide layer were probably caused by growth and thermal stress during in the reactor, dehydration of the oxide layer in the hot cell, or during preparation. The formation of an oxide layer on the AlMg2 cladding occurs due to environmental influences in the reactor such as gamma radiation temperature, environmental pH, and the amount of chloride ions in the reactor cooling water.

ACKNOWLEDGEMENTS

This research had been made possible through DIPA funding 2021. We also thank Anditania Sari Dwi Putri, Setia Permana, and Nofriady Aziz (Directorate for Development of Nuclear Facilities) for the assistance during characterization.

REFERENCES

[1]. P. H. Liem, T. Surbakti, and D. Hartanto, “Kinetics parameters evaluation on the first core of the RSG GAS (MPR-30) using continuous energy Monte Carlo method,” *Progress in Nuclear Energy*, vol. 109, pp. 196–203, 2018. doi: 10.1016/j.pnucene. 2018.08.014.

[2]. I. D. Abdelrazek, M. Naguib Aly, A. A. Badawi, and A. G. Abo Elnour, “Benchmarking RSG-GAS reactor thermal hydraulic data using RELAP5 code,” *Ann Nucl Energy*, vol. 70, pp. 36–43, 2014. doi: 10.1016/j.anucene. 2014.02.023.

[3]. A. B. Ginting and P. H. Liem, “Absolute burnup measurement of LEU silicide fuel plate irradiated in the RSG GAS multipurpose reactor by destructive radiochemical technique,” *Ann Nucl Energy*, vol. 85, pp. 613–620, 2015. doi: 10.1016/j.anucene.2015.06.016.

[4]. S. Pinem, P. H. Liem, T. M. Sembiring, and T. Surbakti, “Fuel element burnup measurements for the equilibrium LEU silicide RSG GAS (MPR-30) core under a new fuel management strategy,” *Ann Nucl Energy*, vol. 98, pp. 211–217, 2016. doi: 10.1016/j.anucene.2016.08.010.

[5]. P. H. Liem, S. Amini, A. G. Hutagaol, and T. M. Sembiring, “Nondestructive burnup verification by gamma-ray spectroscopy of LEU silicide fuel plates irradiated in the RSG GAS multipurpose reactor,” *Ann Nucl Energy*, vol. 56, pp. 57–65, 2013. doi: 10.1016/j.anucene.2013.01.013.

[6]. P. H. Liem, Zuhair, and D. Hartanto, “Sensitivity and uncertainty analysis on the first core criticality of the RSG GAS multipurpose research reactor,” *Progress in Nuclear Energy*, vol. 114, pp. 46–60, Jul. 2019. doi: 10.1016/j.pnucene.2019.03.001.

[7]. D. Hartanto and P. H. Liem, “Analysis of the first core of the Indonesian multipurpose research reactor RSG-GAS using the Serpent Monte Carlo code and the ENDF/B-VIII.0 nuclear data library,” *Nuclear Engineering and Technology*, vol. 52, no. 12, pp. 2725–2732, Dec. 2020. doi: 10.1016/j.net.2020.05.027.

[8]. T. M. Sembiring, S. Pinem, D. Hartanto, and P. H. Liem, “Analysis of the excess reactivity and control rod worth of RSG-GAS equilibrium silicide core using Continuous-Energy Monte Carlo Serpent2 code,” *Ann Nucl Energy*, vol. 154, May 2021. doi: 10.1016/j.anucene.2020.108107.

[9]. S. Soentono, B. Arbie, A. Suripto, J. K. H. A. Zokhim, K. Barat, and M. Prapatan, “Progress of Indonesia RERTR related programs”.

[10]. A. Suripto and A. Mutalib, “RERTR-related program in Indonesia”.

[11]. A. B. Ginting, Suparjo, D. Anggraini, and H. Nasution, “Thermal characteristic of AlMg2 cladding and fuel plates of U3Si2-Al with various uranium loading,” in *Proceeding of the Third Scientific Presentation on Nuclear Fuel Cycle*, 1997.

[12]. A. Kadarjono, “Structure analysis and phase composistion of U-7%Mo-x%Zr (x = 1, 2, 3 wt%) alloys from melting process,” 2010.

[13]. Y. Nampira and dan S. Ismarwanti, “Nondestructive test of post-irradiated U_3Si_2-Al fuel with uranium density of 4,8 g/cm3 and burn up of 20% and 40%,” *Jurnal Teknologi Bahan Nuklir*, vol. 10, no. 2, pp. 53–63, Jun. 2015,

DOI: https://doi.org/10.17146/urania.2022.28.3.6755

[14]. B. Briyatmoko *et al.*, "PIE Technique for high density U3Si2-Al fuel plate," 2015.
[15]. K. Kadarusmanto, P. Purwadi, and E. Susilowati, "Determination of burn-up for testing fuel plate," *Reaktor : Buletin Pengelolaan Reaktor Nuklir*, vol. 13, no. 1, pp. 25–29, Nov. 2017. doi: 10.17146/BPRN.2016.13.1.3882.
[16]. J. C. Sihotang, M. K. Ajiriyanto, A. S. D. Putri, E. Nurlaily, A. B. Ginting, "Study of fission gas bubbles and interaction layer on irradiated U_3Si_2-Al density of 4.8 gU/cm3," *Urania : Jurnal Ilmiah Daur Bahan Bakar Nuklir*, vol. 28, no. 2, pp. 69–78, Jun. 2022. doi:10.17146/URANIA.2022.28.2.6670.
[17]. D. Anggraini, M. Kartaman, R. Kriswarini, and Yanlinastuti, "Corrosion analysis of AlMg2 and AlMgSi using electrochemical method," *Urania : Jurnal Ilmiah Daur Bahan Bakar Nuklir*, vol. 20, no. 3, 2014.
[18]. C. R. F. Azevedo, "Selection of fuel cladding material for nuclear fission reactors," *Eng Fail Anal*, vol. 18, no. 8, pp. 1943–1962, Dec. 2011, doi: 10.1016/J.ENGFAILANAL.2011.06.010
[19]. C. Peng, G. Cao, T. Gu, C. Wang, Z. Wang, and C. Sun, "The corrosion behavior of the 6061 Al alloy in simulated Nansha marine atmosphere," *Journal of Materials Research and Technology*, vol. 19, pp. 709–721, 2022. doi: 10.1016/J.JMRT.2022.05.066.
[20]. F. Bahar, S. Sriyono, and G. R. Sunaryo, "Analysis on AlMg2 as RSG-GAS cladding material corrosion in chloride containing water," *GANENDRA Majalah IPTEK Nuklir*, vol. 21, no. 2, pp. 83–88, Oct. 2018. doi: 10.17146/GND.2018.21.2.4271.
[21]. Y. S. Kim, G. L. Hofman, A. B. Robinson, J. L. Snelgrove, and N. Hanan, "Oxidation of aluminum alloy cladding for research and test reactor fuel," *Journal of Nuclear Materials*, vol. 378, no. 2, pp. 220–228, Aug. 2008. doi: 10.1016/J.JNUCMAT.2008.06.032.
[22]. A. Leenaers *et al.*, "Microstructure of U3Si2 fuel plates submitted to a high heat flux," *Journal of Nuclear Materials*, vol. 327, no. 2–3, pp. 121–129, 2004. doi: 10.1016/J.JNUCMAT.2004.01.025.
[23]. A. Leenaers, *et al.* "Post-irradiation examination of AlFeNi cladded U3Si2 fuel plates irradiated under severe conditions," *Journal of Nuclear Materials*, vol. 375, no. 2, pp. 243–251, 2008. doi: 10.1016/J.JNUCMAT.2008.01.013.
[24]. R. Artika *et al.*, "Non-destructive test for U_3Si_2/Al fuel plate with 4,8 gU/cm^3 uranium density using digital X-ray radiography," *Urania : Jurnal Ilmiah Daur Bahan Bakar Nuklir*, vol. 25, no. 1, pp. 49–56, 2020.
[25]. A. B. Ginting, et. al, "Burn-up calculation of the middle part of irradiated U_3Si_2/Al fuel plate with 4.8 gU/cm^3 density," *Urania : Jurnal Ilmiah Daur Bahan Bakar Nuklir*, vol. 26, no. 2, pp. 31–36, 2020. doi:10.17146/URANIA.2020.26.2.5864.
[26]. M. Wintergerst, *et al.*, "Corrosion of the AlFeNi alloy used for the fuel cladding in the Jules Horowitz research reactor," *Journal of Nuclear Materials*, vol. 393, no. 3, pp. 369–380, Sep. 2009. doi: 10.1016/J.JNUCMAT.2009.06.003.
[27]. S. K. Sen *et al.*, "Gamma-radiation-induced corrosion of aluminum alloy: low dose effect," *J Phys Conf Ser*, vol. 860, no. 1, p. 012041, Jun. 2017. doi: 10.1088/1742-6596/860/1/012041.

THIS PAGE INTENTIONALLY LEFT BLANK

DOI: https://doi.org/10.17146/urania.2022.28.3.6755